Contribution from the Chemistry Division,
Argonne National Laboratory, Argonne, Illinois 60439

Structural Studies of Precursor and Partially Oxidized Conducting Complexes. 20. A Reduction in Platinum-Chain Dimerization in Rubidium Tetracyanoplatinate Chloride (2:1:0.3) Trihydrate, $Rb_2[Pt(CN)_4]Cl_{0.3}\cdot 3.0H_2O$, at 110 K As Revealed by a Neutron Diffraction Study[1]

RICHARD K. BROWN and JACK M. WILLIAMS*

Received December 27, 1978

The crystal and molecular structure of the partially oxidized tetracyanoplatinate (POTCP) complex $Rb_2[Pt(CN)_4]Cl_{0.3}\cdot 3H_2O$ has been studied at low temperature (T = 110 K) to determine if the degree of Pt-chain dimerization observed at 298 K remains constant. Crystals of the complex are tetragonal (space group $P4mm$) with unit cell dimensions a = 10.104 (4) Å, c = 5.743 (2) Å, and V_c = 586.3 Å^3 for Z = 2. A 1.74% decrease in cell volume was observed upon cooling from 298 to 110 K. For the derivation of very high-precision structural parameters, a replicate data set of 1183 reflections was collected and averaged to yield 586 independent data of which 539 had $F_o^2 > \sigma(F_o^2)$. The structure was refined by full-matrix least-squares techniques to final $R(F_o^2)$ and $R_w(F_o^2)$ values of 0.056 and 0.077, respectively. A decrease in both the average Pt–Pt spacing (~0.2 Å to 2.87 Å) and, unexpectedly, the degree of dimerization [Pt–Pt(110 K) = 2.862 (6) and 2.885 (6) Å vs. 2.877 (8) and 2.924 (8) Å at 298 K] is observed at 110 K. However, the electrical conductivity of this complex, which might be expected to increase with decreased Pt-chain dimerization, falls off rapidly with decreasing temperature. These seemingly contradictory observations are discussed, and the temperature-dependent electrical conductivity is interpreted within the framework of a Peierls metal–insulator transition. We also present a new interpretation of the possible correlation between the degree of partial oxidation (DPO) of the platinum atoms in POTCP salts and the presence of Pt–Pt intrachain dimerization.

Introduction

We have recently reported the crystal and molecular structures of several newly synthesized, one-dimensional (1-D), partially oxidized tetracyanoplatinate (POTCP) complexes.[2-10] The main stimulus for these studies is Little's prediction that high-temperature excitonic superconductivity might originate in certain 1-D type metals.[11] Electron transport in these complexes occurs along the 1-D Pt atom chain, the latter resulting from the columnar stacking of the square-planar $[Pt(CN)_4]^{x-}$ groups and concomitant d_{z^2} orbital overlap. The Pt–Pt spacings are often only ~0.01–0.3 Å longer than in Pt metal (2.78 Å).

Room-temperature electrical conductivities[12] of several 1-D POTCP complexes indicate that the shorter and more nearly equal the Pt–Pt separations in the chain, the higher the electrical conductivity. This point is illustrated by comparison of the electrical conductivities of several isostructural POTCP salts with those of the prototypical complexes $K_2[Pt(CN)_4]X_{0.3}\cdot 3H_2O$ (X = Br or Cl), KCP(Br) or KCP(Cl) hereafter, respectively. The complexes $(NH_4)_2[Pt(CN)_4]Cl_{0.3}\cdot 3H_2O$[7] and $Rb_2[Pt(CN)_4]Cl_{0.3}\cdot 3H_2O$,[6] $NH_4CP(Cl)$ and RbCP(Cl) hereafter, respectively, and KCP(Br)[2] all crystallize in the tetragonal space group $P4mm$ which in itself does not require equivalence of the *intra*chain Pt–Pt spacings. That is, dimerization is possible, yielding alternately short and long Pt–Pt separations, which could cause electron localization (decreased electrical mobility) along the Pt atom chain. This dimerization is observed in $NH_4CP(Cl)$[7] and RbCP(Cl)[6] where the room-temperature Pt–Pt separations are 2.910 (5) and 2.930 (5) Å, and 2.877 (8) and 2.924 (8) Å, respectively. For KCP(Br) the Pt–Pt separations are *equal* at 2.88 (1) Å. In accordance with these intrachain separations, the trend in room-temperature electrical conductivities is KCP(Cl) > RbCP(Cl) > $NH_4CP(Cl)$.[12] Room-temperature conductivity studies of anhydrous $Cs_2[Pt(CN)_4](FHF)_{0.39}$ and $Rb[Pt(CN)_4](FHF)_{0.40}$ (CsCP(FHF) and RbCP(FHF) hereafter, respectively), which crystallize in the tetragonal space group $I4/mcm$ requiring equivalent Pt–Pt spacings [Pt–Pt = 2.833 (1) and 2.798 (1) Å, respectively], have also recently been reported.[4,13] As expected, the short Pt atom spacing leads to a room-temperature electrical conductivity approximately triple (~2000 Ω^{-1} cm^{-1}) the maximum reported for KCP(Br).[12]

Temperature-dependent conductivity measurements have also been reported for KCP(Br), $NH_4CP(Cl)$, and RbCP(Cl)[12] and indicate a drastic decrease in electrical conductivity with decreased temperature for all three complexes. This is contrary to what one might expect assuming a uniform contraction in the Pt–Pt spacing with diminished temperature. Therefore, we have reexamined the crystal and molecular structure of RbCP(Cl) at 110 K in order to precisely determine the structural modifications which occur and may in turn affect the electrical conductivity.

Experimental Section

A description of the synthesis, crystal preparation and space group determination for RbCP(Cl) appears elsewhere.[6]

Data Collection. A well-formed 10-mg crystal of RbCP(Cl) was sealed in a lead-glass capillary to protect against dehydration. The crystal was mounted with the crystallographic c axis coincident with the instrument ϕ axis of an Electronics-and-Alloys four-circle automated diffractometer at the Argonne CP-5 reactor. The temperature at the crystal was maintained at 110 K with a N_2 gas flow system of the Strouse design.[14] From a least-squares fit of the setting angles of 26 intense reflections with $40° < 2\theta < 85°$ (λ 1.142 (1) Å), the following unit cell constants ($P4mm$) were derived: a = 10.104 (4) Å, c = 5.743 (2) Å, V_c = 586.3 Å^3 for Z = 2.

Based on the least-squares-determined orientation matrix, data were collected automatically by using the θ–2θ step-scan method with 0.1° step intervals and preset scan ranges of 41–67 steps. At each extremity of the scan the background intensities were established with both crystal and detector in a stationary position. The total number of data collected was 1183 (586 independent) to $(\sin\theta)/\lambda = 0.724$ Å^{-1}. Of the 586 independent data, 539 had $F_o^2 > \sigma F_o^2$. Instrument and crystal stabilities were monitored by remeasuring two reference reflections after every 80 regular data, and their combined intensity did not vary more than 5% during data collection. Individual reflections were corrected for absorption (μ_{calcd} = 1.16 cm^{-1}), and the calculated transmission factors ranged from 0.84 to 0.90. With the use of the absorption-corrected integrated intensities, the F_o^2 values were obtained in the usual manner.[6] All variances of F_o^2 were calculated from $\sigma^2(F_o^2) = \sigma_c^2(F_o^2) + (0.05F_o^2)$, where $\sigma_c(F_o^2)$ was determined from the counting statistics, and the second term was added to account for errors other than those arising from counting statistics.

Structure Solution and Refinement. Initial coordinates for all atoms were obtained from the room-temperature neutron diffraction study.[6]

0020-1669/79/1318-1922$01.00/0

Table I. Positional and Thermal Parameters (Å²) (T = 110 K) for $Rb_2[Pt(CN)_4]Cl_{0.3}\cdot 3.0H_2O$[a]

atom	x	y	z	U_{11}	U_{22}	U_{33}	U_{12}	U_{13}	U_{23}
Pt(1)	0.0	0.0	0.0	0.010 (1)	0.010	0.006 (1)	0.0	0.0	0.0
Pt(2)	0.0	0.0	0.4980 (10)	0.010 (1)	0.010	0.007 (1)	0.0	0.0	0.0
C(1)	0.1976 (2)	0.0	−0.0038 (11)	0.013 (1)	0.016 (1)	0.011 (1)	0.0	−0.001 (1)	0.0
C(2)	0.1399 (2)	0.1399	0.5003 (10)	0.013 (1)	0.013	0.013 (1)	−0.003 (1)	0.001 (2)	0.001
N(1)	0.3121 (1)	0.0	−0.0095 (10)	0.012 (1)	0.029 (1)	0.020 (1)	0.0	0.002 (1)	0.0
N(2)	0.2209 (2)	0.2209	0.5062 (10)	0.020 (1)	0.020	0.022 (1)	−0.007 (1)	−0.001 (2)	−0.001
Cl	0.5000	0.5000	0.4833 (17)	0.014 (3)	0.014	0.017 (3)	0.0	0.0	0.0
Rb	0.1978 (2)	0.5000	0.7389 (11)	0.023 (1)	0.019 (1)	0.028 (1)	0.0	−0.002 (1)	0.0
O(1)	0.5000	0.0	0.3813 (11)	0.019 (2)	0.049 (3)	0.017 (2)	0.0	0.0	0.0
O(2)	0.3389 (7)	0.3389	0.0862 (11)	0.047 (3)	0.047	0.035 (2)	0.008 (2)	0.011 (3)	0.011
H(1)	0.4264 (7)	0.0	0.2772 (15)	0.036 (3)	0.070 (5)	0.038 (4)	0.0	−0.012 (3)	0.0
H(2)	0.2878 (18)	0.2878	0.1808 (26)	0.075 (8)	0.075	0.110 (10)	0.013 (6)	0.038 (12)	0.038
H(3)	0.3861 (18)	0.3861	0.2034 (20)	0.117 (14)	0.117	0.057 (6)	−0.020 (9)	−0.016 (10)	−0.016

[a] Thermal parameters correspond to the expression $T = -[8\pi^2(U_{11}h^2a^{*2} + \ldots + 2U_{12}hka^*b^* + \ldots)]$. Estimated standard deviations are given in parentheses. Values for which no esd is given were held constant, due to symmetry constraints, during least-squares refinement.

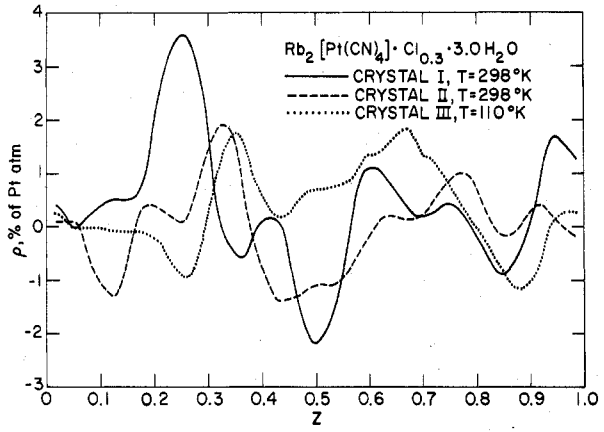

Figure 1. Difference Fourier density line (0.5, 0.5, z) from the neutron data. Possible "second sites" at $z \simeq 0.35$ and 0.67 could not be confirmed from least-squares analysis (see text).

Three cycles of full-matrix, isotropic refinement using all 586 independent data led to

$$R(F_o) = (\Sigma||F_o| - |F_c||)/\Sigma|F_o| = 0.097$$

$$R(F_o^2) = \Sigma|F_o^2 - F_c^2|/\Sigma F_o^2 = 0.134$$

$$R_w(F_o^2) = [\Sigma w|F_o^2 - F_c^2|^2/\Sigma w_i F_o^4]^{1/2} = 0.180$$

By use of anisotropic temperature factors and an isotropic extinction correction (Zachariasen[15,16]), several cycles of full-matrix least-squares refinement led to values for $R(F_o)$, $R(F_o^2)$, and $R_w(F_o^2)$ of 0.051, 0.056, and 0.077, respectively.

The standard deviation of an observation of unit weight, $\sigma_1 = [w_i|F_o^2 - F_c^2|^2/(np)]^{1/2}$ where n is the number of observations and p the number of parameters varied (69) in the least-squares refinement, was 1.21. Final positional and thermal parameters are given in Table I. The final observation to parameter ratio was 8.5:1. In the final cycle of refinement the largest shift to error ratio was 0.11.

A final difference Fourier map showed two positive peaks at ~2.5 times background level at $^1/_2$, $^1/_2$, 0.35 and $^1/_2$, $^1/_2$, 0.67 which correspond to residual density peaks also found in the room-temperature neutron study.[6] These could correspond to "defect water" sites as reported for KCP(Br).[2] Attempts to locate hydrogen atoms near either of the two sites failed, and attempts to refine these positions by least-squares techniques invariably led to nonpositive definite temperature factors. It is therefore likely, by analogy[2] with KCP(Cl) and KCP(Br), that Cl^- or H_2O or both alternately occupy these sites. We are certain, however, that the existence of these sites is not an artifact of the data, since these peaks have now been observed in two independent room-temperature neutron diffraction studies[6] and in the present 110 K neutron data set by using a third crystal. Finally we note that the peak found at ($^1/_2$, $^1/_2$, 0.67) occurs at nearly the same position found for the "second site" in KCP(Br)[2] and $NH_4CP(Cl)$[7] as displayed in Figure 1.

Table II. Selected Distances (Å) and Angles (deg) (T = 110 K) for $Rb_2[Pt(CN)_4]Cl_{0.3}\cdot 3.0H_2O$[a]

(A) Distances around Platinum Atoms

Pt(1)–Pt(2)	2.862 (6) [2.877 (8)][b]	Pt(1)–Pt(2)^{I}	2.885 (6) [2.924 (8)]
Pt(1)–C(1)	1.998 (2) [1.999 (2)]	Pt(2)–C(2)	2.001 (2) [2.005 (2)]

(B) C–N Distances in Cyanide Groups

C(1)–N(1)	1.158 (2) [1.155 (3)]	C(2)–N(2)	1.159 (2) [1.149 (3)]

(C) Water Molecule Distances[c]

O(1)–H(1)	0.955 (7), 0.982 (8) [0.946 (10), 0.970 (11)]
O(2)–H(2)	0.910 (13), 0.989 (15) [0.873 (17), 0.969 (23)]
O(2)–H(3)	0.954 (12), 1.025 (14) [0.859 (25), 0.958 (28)]

(D) Hydrogen Atom Interactions

H(1)···N(1)	2.013 (7) [2.034 (9)]	O(1)–H(1)···N(1)	163.8 (7) [164.6 (9)]
H(2)···N(2)	2.100 (12) [2.149 (16)]	O(2)–H(2)···N(2)	153.8 (15) [153.5 (18)]
H(3)···Cl	2.289 (11) [2.401 (21)]	O(2)–H(3)···Cl	179.7 (11) [179.8 (16)]

(E) Rubidium Ion Interactions

Rb–O(1)^{II}	2.868 (5) [2.895 (7)]	Rb–N(2)^{o,VII}	3.132 (2) [3.160 (3)]
Rb–O(2)^{III,IV}	2.945 (5) [2.985 (9)]	Rb–Cl	3.391 (4) [3.391 (7)]
Rb–N(1)^{V,VI}	3.115 (3) [3.128 (3)]		

(F) Chloride Ion Interactions

Cl–O(2)^{o,VII,VIII,IX}	3.243 (8) [3.260 (14)]	Cl–Rb^{o,II,VIII,X}	3.391 (4) [3.391 (7)]

(G) Angles of Pt Chain and Bonded Atoms

Pt(2)–Pt(1)–Pt(2)^{I}	180 [180]
Pt(1)–C(1)–N(1)	179.0 (4) [179.3 (5)]
Pt(2)–C(2)–N(2)	178.7 (4) [179.6 (5)]
C(1)–Pt(1)–C(1)^{II}	89.993 (4) [89.99 (1)]
C(2)–Pt(2)–C(2)^{XI}	90.00 (1) [89.99 (1)]
H(1)–O(1)–H(1)^{V}	102.4 (10) [101.9 (14)]
H(2)–O(2)–H(3)	98.4 (13) [99.1 (17)]

[a] Standard deviations of the least significant digits are given in parentheses. Superscripts refer to symmetry positions. If zero (0) or no superscript appears (x, y, z) is implied: (I) x, y, $z-1$; (II) y, x, z; (III) x, y, $z+1$; (IV) x, $1-y$, $z+1$; (V) y, x, $z+1$; (VI) $-y$, $1-x$, $z+1$; (VII) x, $1-y$, z; (VIII) $1-x$, $1-y$, z; (IX) $1-x$, $-y$, z; (X) $1-y$, $1-x$, z; (XI) $-x$, $-y$, z. [b] Values in brackets refer to the room-temperature structure and are included for comparative purposes. [c] Corrected for thermal motion; hydrogen assumed to ride on oxygen.

Results and Discussion

Important bond distances and angles for RbCP(Cl) are given in Table II. As is the case for previously studied

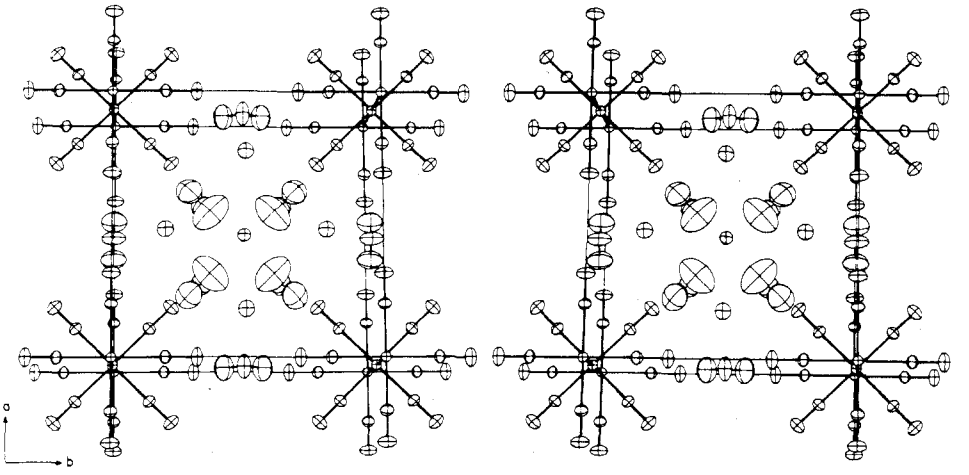

Figure 2. Stereo drawing of the structure of tetragonal $Rb_2[Pt(CN)_4]Cl_{0.3}\cdot 3.0H_2O$ as viewed down *c*. The linear Pt atom chain is parallel to *c*. The *single* confirmed Cl^- site is located in the center of each stereopair. All ellipsoids are scaled to 50% probability.

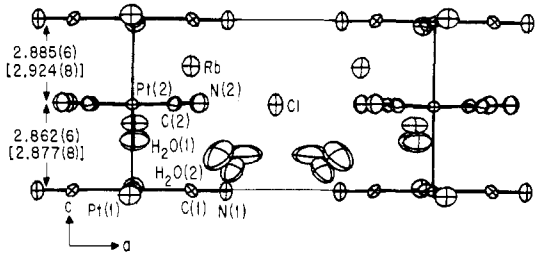

Figure 3. Drawing of the unit cell (50% probability ellipsoids) of $Rb_2[Pt(CN)_4]Cl_{0.3}\cdot 3.0H_2O$ showing the linear Pt atom chain, which contains *un*equal Pt–Pt separations, and the asymmetric location of the Rb^+ ion and the H_2O molecules. Distances are in angstroms, and values in brackets refer to the room-temperature structure.[6]

anion-deficient 1-D POTCP complexes, the structure consists of perfectly linear Pt atom chains which in this case arise from the columnar stacking of square-planar $Pt(CN)_4^{1.7-}$ moieties. This stacking occurs along the tetragonal *c* axis as shown in Figures 2 and 3.

As mentioned in the Introduction, RbCP(Cl) belongs to the acentric space group *P4mm* which permits nonequivalence of intrachain Pt–Pt separations. A most significant finding of the low-temperature study is that the difference in Pt–Pt separations at room temperature is 0.047 (11) Å whereas at 110 K it is diminished by ~50% to only 0.023 (8) Å. The total decrease in the *c*-axis length upon passing from 298 to 110 K is 0.054 (4) Å, and of this 0.015 Å may be ascribed to a decrease in the Pt–Pt separation between the two Pt atoms with the smaller separation while the remaining 0.039 Å involves a similar decrease between the Pt atoms with the larger separation. Thus the overall effect is a diminution in the Pt atom chain dimerization. However, the electrical conductivity at 110 K, which might be expected to increase with decreased chain dimerization, is considerably less than at 298 K.[12] This observation appears to conflict with those mentioned previously, which were made for several 1-D POTCP materials at room temperature where it was found that as Pt–Pt spacings decrease the electrical conductivity generally increases. However, there appears to be a fundamental difference between comparison of observations involving several different complexes, all at room temperature, and comparison of those from an individual complex over a temperature range. The important point is that a metallic state apparently exists above the Peierls transition temperature, but that upon decreasing the temperature a transition to a low-temperature insulating state eventually occurs.[17] In 1973 Comes et al.[18] observed, from X-ray diffuse scattering experiments, that some phase correlation existed between the distortions in neighboring chains in KCP(Br) at 77 K. Renker et al.[19] have also observed incomplete three-dimensional ordering between 80 and 120 K for KCP(Br). In view of these findings and the fact that RbCP(Cl) and KCP(Br) are isostructural, it seems likely that the transition to the insulating state is at least partially complete at 110 K for RbCP(Cl). Therefore, the electrical conductivity decreases with temperature even though the intrachain Pt–Pt spacings, and degree of chain dimerization, are diminished.

Although the contraction in Pt–Pt separations with decreased temperature is to be expected, the cause of the decrease in degree of dimerization is not obvious.[20] Even though the Rb–N(2) interaction (see Figure 10 of ref 6) is shortened by 0.028 (4) Å, whereas Rb–N(1) is shortened by only 0.013 (4) Å, it is difficult to ascribe this small and perhaps insignificant effect as the sole cause of the decrease in dimerization. It seems likely that the asymmetric distribution of cations and water molecules in the crystal lattice, i.e., the type of crystal structure formed, plays a rather significant role in the dimerization of the Pt–Pt chain. This seems especially likely in light of the fact that all POTCP complexes which have crystallographically equivalent Pt–Pt spacings also have the cations constrained to share the same plane as the $Pt(CN)_4$ groups [i.e., RbCP(FHF),[4] CsCP(FHF),[5] $Cs_2[Pt(CN)_4]Cl_{0.3}$,[9] and $Cs_2[Pt(CN)_4](N_3)_{0.25}\cdot{}^1/_2H_2O$][22] and do not have H_2O sites independent of the anion sites.[23] These latter complexes crystallize in the space group $I4/mcm$, or the nearly identical space group $P\bar{4}b2$, with $Z = 4$ and unit cell volumes approximately twice those of the complexes which crystallize in *P4mm*. Hence, not all of the 1-D POTCP complexes being considered here are strictly isomorphous. The 3-D structure of the two types of systems, however, is very similar. To demonstrate this we should point out the simple relationship between *P4mm* and $I4/mcm$, i.e., the complexes which crystallize in $I4/mcm$ or $P\bar{4}b2$ have unit cell dimensions of a or $b \approx 13$ Å and $c \approx 5.9$ Å. This cell can be operated upon with the transformation matrix

$$\begin{bmatrix} -1/2 & 1/2 & 0 \\ 1/2 & 1/2 & 0 \\ 0 & 0 & 1 \end{bmatrix}$$

to yield a cell with dimensions of a or $b \approx 10$ Å and $c \approx 5.9$ Å, which is nearly identical in both size and atom distribution to the *P4mm* cell. The *true* crystallographic symmetry of the two space groups is, of course, different.

As mentioned previously, the only significant difference between these different structure types is the distribution of

cations and H_2O molecules in the crystal lattice. The interchain Pt–Pt separations and $Pt(CN)_4$ torsional angles are nearly the same. Both RbCP(Cl)[6] and $NH_4CP(Cl)$[7] have the same cation and H_2O distribution as that for KCP(Br), yet the Pt–Pt spacings in KCP(Br) are all equal and those in RbCP(Cl) and $NH_4CP(Cl)$ are dimerized.[25] As we have already pointed out, at 298 K RbCP(Cl) has both a larger average Pt–Pt separation and a larger degree of dimerization than at 110 K. However, at 110 K the average Pt–Pt spacing is nearly identical to that for KCP(Cl),[2] which does not exhibit intrachain Pt–Pt dimerization.[2] The only significant difference between these isomorphous 1-D POTCP complexes is the cation radius (r^+). Another interesting observation is that $RbCP(FHF)_{0.4}$, with a very short Pt–Pt spacing of 2.798 (1) Å, is not dimerized.[4] In light of these observations it becomes tempting to speculate that the presence of dimerization is dependent in some manner on the average Pt–Pt separation and on (r^+).

We can summarize these observations as follows: (1) for a given Pt–Pt spacing, as r^+ increases the likelihood of dimerization increases, and (2) for a given r^+, as the Pt–Pt spacing decreases the likelihood that dimerization will occur decreases. As has been shown previously,[9] for a given r^+ the Pt–Pt spacing tends to depend on the degree of partial oxidation (DPO). Therefore, one might conclude that the degree of Pt–Pt chain dimerization is also indirectly dependent on the DPO. If this is truly the case, then the reversal of chain dimerization between RbCP(Cl) and $NH_4CP(Cl)$ becomes significantly less important.[25] It now appears that we have a framework within which it is possible to rationalize why only some Pt–Pt chains are dimerized and to correlate the DPO with both the magnitude of Pt–Pt separations and presence of dimerization. Research efforts to date have concentrated on obtaining POTCP complexes with the shortest possible Pt–Pt spacings, hence the number of complexes displaying dimerized chains is very limited. It is our hope that continuing investigations of POTCP complexes will provide us with more definitive information about the correlations discussed above.

Acknowledgment. J.M.W. acknowledges NATO (Grant No. 1276), which has made it possible to exchange information with foreign scientists on many occasions, and to Professor A. E. Underhill (Bangor, Wales) for providing conductivity results prior to publication.

Supplementary Material Available: Listing of nuclear structure factors (4 pages). Ordering information is given on any current masthead page.

References and Notes

(1) Research performed under the auspices of the Division of Basic Energy Sciences of the U.S. Department of Energy.
(2) J. M. Williams, J. L. Petersen, H. M. Gerdes, and S. W. Peterson, *Phys. Rev. Lett.*, **33**, 1079 (1974); G. Heger, H. J. Deiseroth, and H. Schultz, *Acta Crystallogr., Sect. B*, **34**, 725 (1978); C. Peters and C. F. Eagen, *Inorg. Chem.*, **15**, 782 (1976).
(3) J. M. Williams, K. D. Keefer, D. M. Washecheck, and N. P. Enright, *Inorg. Chem.*, **15**, 2446 (1976).
(4) A. J. Schultz, C. C. Coffey, G. C. Lee, and J. M. Williams, *Inorg. Chem.*, **16**, 2129 (1977).
(5) A. J. Schultz, D. P. Gerrity, and J. M. Williams, *Acta Crystallogr., Sect. B*, **34**, 1673 (1978).
(6) J. M. Williams, P. L. Johnson, and A. J. Schultz, and C. C. Coffey, *Inorg. Chem.*, **17**, 834 (1978).
(7) P. L. Johnson, A. J. Schultz, A. E. Underhill, D. M. Watkins, D. J. Wood, and J. M. Williams, *Inorg. Chem.*, **17**, 839 (1978).
(8) R. K. Brown, P. L. Johnson, T. J. Lynch, and J. M. Williams, *Acta Crystallogr., Sect. B*, **34**, 1965 (1978).
(9) R. K. Brown and J. M. Williams, *Inorg. Chem.*, **17**, 2607 (1978).
(10) J. M. Williams and A. J. Schultz in "Molecular Metals", W. E. Hatfield, Ed., Plenum Press, New York, 1979, pp 337–368.
(11) W. A. Little, *Phys. Rev. A*, **134**, 1416 (1964); *Sci. Am.*, **212**, 21 (Feb 1965).
(12) A. E. Underhill, D. M. Watkins, and D. J. Wood, *J. Chem. Soc., Chem. Commun.*, 805 (1976); J. M. Williams and A. J. Schultz, unpublished results.
(13) J. M. Williams, D. P. Gerrity and A. J. Schultz, *J. Am. Chem. Soc.*, **99**, 1668 (1977); J. M. Williams, A. J. Schultz, K. B. Cornett, and R. E. Besinger, *ibid.*, **100**, 5572 (1978).
(14) C. E. Strouse, *Rev. Sci. Instrum.*, **47**, 871 (1976).
(15) W. H. Zachariasen, *Acta Crystallogr., Sect. A*, **24**, 421 (1967).
(16) P. Coppens and W. C. Hamilton, *Acta Crystallogr., Sect. A*, **26**, 71 (1970).
(17) B. Renker and R. Comes in "Low Dimensional Cooperative Phenomena", H. J. Keller, Ed., Plenum Press, New York, 1975, p 235.
(18) R. Comes, M. Lambert, H. Launois, and H. R. Zeller, *Phys. Rev.*, **38**, 571 (1973).
(19) B. Renker, L. Pintschovius, W. Glaser, H. Rietschel, R. Comes, L. Liebert, and W. Drexel, *Phys. Rev. Lett.*, **32**, 836 (1974).
(20) The atomic-scale Pt-chain dimerization observed from the elastic neutron scattering of the normal tetragonal lattice should not be confused with the previous observation, in KCP(Br), of a sinusoidal displacement of 0.026 Å at 7 K of the $Pt(CN)_4$ groups in response to a charge density wave (CDW) instability. The latter observation was made by neutron-scattering examination of very weak satellite reflections.[21]
(21) C. F. Eagen, S. A. Werner, and R. B. Saillant, *Phys. Rev. B*, **12**, 2036 (1975); J. W. Lynn, M. Iizumi, G. Shirane, S. A. Werner, and R. B. Saillant, *Phys. Rev. B*, **12**, 1154 (1975).
(22) R. K. Brown and J. M. Williams, *Inorg. Chem.*, **18**, 801 (1979).
(23) From electrical conductivity studies, Underhill et al. have observed that the temperature at which three-dimensional ordering occurs (T_{3D}) between the platinum chains depends to a large extent on the presence or absence of a hydrogen-bonded network of ions or molecules cross-linking the platinum atom chains.[24]
(24) A. E. Underhill and D. J. Wood, *Ann. N. Y. Acad. Sci.*, **313**, 516 (1978); D. J. Wood, A. E. Underhill, A. J. Schultz, and J. M. Williams, submitted for publication in *Solid State Commun.*; A. E. Underhill and K. Carneiro, private communication.
(25) The fact that the order of alternately long and short Pt–Pt separations in RbCP(Cl) is reversed as compared to that for $NH_4CP(Cl)$ may well be due to the hydrogen-bonding characteristics of the NH_4^+ cation.[7]